Fish Physiol Biochem (2017) 43:385–395
DOI 10.1007/s10695-016-0294-3

Characterization of *pax3a* and *pax3b* genes in artificially induced polyploid and gynogenetic olive flounder (*Paralichthys olivaceus*) during embryogenesis

Shuang Jiao · Zhihao Wu · Xungang Tan · Yulei Sui · Lijuan Wang · Feng You

Received: 3 May 2016 / Accepted: 21 September 2016 / Published online: 27 September 2016

Abstract Although chromosome set manipulation techniques including polyploidy induction and gynogentic induction in flatfish are becoming increasingly mature, there exists a poor understanding of their effects on embryonic development. PAX3 plays crucial roles during embryonic myogenesis and neurogenesis. In olive flounder (*Paralichthys olivaceus*), there are two duplicated *pax3* genes (*pax3a*, *pax3b*), and both of them are expressed in the brain and muscle regions with some subtle regional differences. We utilized *pax3a* and *pax3b* as indicators to preliminarily investigate whether chromosome set manipulation affects embryonic neurogenesis and myogenesis using whole-mount in situ hybridization. In the polyploid induction groups, 94 % of embryos in the triploid induction group had normal *pax3a/3b* expression patterns; however, 45 % of embryos in the tetraploid induction group showed abnormal *pax3a/3b* expression patterns from the tailbud formation stage to the hatching stage. Therefore, the artificial induction of triploidy and tetraploidy had a small or a moderate effect on flounder embryonic myogenesis and neurogenesis, respectively. In the gynogenetic induction groups, 87 % of embryos in the meiogynogenetic diploid induction group showed normal *pax3a/3b* expression patterns. However, almost 100 % of embryos in the gynogenetic haploid induction group and 63 % of embryos in the mitogynogenetic diploid induction group showed abnormal *pax3a/3b* expression patterns. Therefore, the induction of gynogenetic haploidy and mitogynogenetic diploidy had large effects on flounder embryonic myogenesis and neurogenesis. In conclusion, the differential expression of *pax3a* and *pax3b* may provide new insights for consideration of fish chromosome set manipulation.

Keywords Gynogenetic induction group · Olive flounder (*Paralichthys olivaceus*) · *pax3a* · *pax3b* · Triploid induction group · Tetraploid induction group

Electronic supplementary material The online version of this article (doi:10.1007/s10695-016-0294-3) contains supplementary material, which is available to authorized users.

S. Jiao · Z. Wu · X. Tan · Y. Sui · L. Wang · F. You
Key Laboratory of Experimental Marine Biology, Institute of Oceanology, Chinese Academy of Sciences, 7 Nanhai Road, Qingdao 266071, Shandong, People's Republic of China

S. Jiao · Z. Wu · X. Tan · Y. Sui · L. Wang · F. You (✉)
Laboratory for Marine Biology and Biotechnology, Qingdao National Laboratory for Marine Science and Technology, 7 Nanhai Road, Qingdao 266071, Shandong, People's Republic of China
e-mail: youfeng@qdio.ac.cn

Y. Sui · L. Wang
University of Chinese Academy of Sciences, Beijing 100049, People's Republic of China

Introduction

The induction of triploidy and gynogenesis by chromosome set manipulation plays more and more important roles in modern fish breeding. Most artificial triploid fish are sterile, promoting growth rate and food conversion rate. Also, the production of sterile triploids could prevent the interaction between farmed and wild fish. In addition to inducing triploids through suppression of the second polar body release, they can also be produced by intercrossing tetraploids with diploids. The tetraploid fish are usually induced through suppression of the first mitotic division by physical methods (Xu et al. 2015). On the other hand, artificial gynogenesis has been proven to be a valuable genetic tool in the rapid establishment of inbred or pure lines, the production of all-female stocks, the investigation of sex determination mechanisms, and the mapping of genes (Molina-Luzon et al. 2015). The gynogenetic diploids are induced by first using irradiated sperm to fertilize normal eggs and then suppressing the second meiotic division of these eggs (meiogynogenetic diploids) or the first mitotic division of the zygotes (mitogynogenetic diploids) (Felip et al. 2001).

There are studies that show chromosome set manipulation may have an effect on neurogenesis and myogenesis. Artificially induced haploid embryos of amphibians and fish developed the typical haploid syndrome, displaying impaired neural development, short myotomes and poor muscle differentiation (Hamilton 1963, 1966; Purdom 1969; Uwa 1965). In goldfish (*Carassius auratus*), some proteins correlative with neural development were significantly different between haploid embryos and diploid embryos (Huang et al. 2004). In Atlantic salmon (*Salmo salar* L.), myogenesis and neuromuscular development occurred at slightly earlier somite stages in triploids than in diploids (Johnston et al. 1999). In juvenile rainbow trout (*Oncorhynchus mykiss*), polyploidy influenced the expression of genes critical to muscle development and general growth regulation, which may explain why triploid fish recovered from nutritional insult better than diploid fish (Cleveland and Weber 2014).

The olive flounder (*Paralichthys olivaceus*) is one of the most economically important marine fish for aquaculture on the northern coast of China due to its high demand in the international and domestic market (Li et al. 2015). To improve growth rates and shorten culture periods, research on chromosome set manipulation, including the induction of triploidy and gynogenesis, has been performed. However, most studies have focused on finding suitable methods to induce triploidy or gynogenesis and have been limited to morphological descriptions of their embryonic development and early growth by direct observation (Liu et al. 2008; Xu and Chen 2010; Yi et al. 2012; You and Liu 1995; You et al. 2001). Thus, there is considerable interest in the development of molecular biology methods for detecting the effects of flounder chromosome set manipulations on embryogenesis. Neurogenesis and myogenesis are the processes involved in neural and muscle development, respectively. *Pax3* is an evolutionarily conserved transcription factor and has been proven to play roles in both neurogenesis and myogenesis (Buckingham and Relaix 2015; Lang et al. 2007). During mouse embryonic development, *Pax3* is expressed in the dorsal neural tube, the neural crest and the presomitic mesoderm as somites are formed, and progressively restricted to the dermomyotome as somites mature. *Splotch* (*Sp*) mice, in which a mutation disrupts Pax3 function, have defects in dorsal neural tube closure, neural crest cell migration, and somitogenesis (Relaix et al. 2004; Schubert et al. 2001; Tremblay et al. 1995). Besides, during zebrafish embryogenesis, the expression patterns of *pax3a* and *pax3b* are very similar to their murine homologues (Minchin and Hughes 2008; Minchin et al. 2013; Seo et al. 1998). In flounder, there are two duplicated genes, *pax3a* and *pax3b*, with different expression patterns. Both of them are expressed in the developing nervous system with slightly regional differences during early neurogenesis. Moreover, their mRNA signals can also be detected in the somite region, with *pax3a* scattered in the somites and *pax3b* expressed in the newly forming somites (Jiao et al. 2015). Thus, *pax3a* and *pax3b* signals can be used as indicators of embryonic neurogenensis and myogenesis.

In the present study, we mainly compared the expression patterns of *pax3a* and *pax3b* genes in artificially induced polyploid and gynogenetic olive flounder during embryogenesis using whole-mount in situ hybridization. From *pax3a* and *pax3b* expression, we preliminarily characterized the effects of ploidy- and gynogenetic-manipulation on embryonic neurogenensis and myogenesis, which provides a

valuable reference for theoretical research on optimizing these induced conditions.

Materials and methods

Ethics statement

Experiments involving flounder were conducted according to the regulations of local and central governments and approved by the Institutional Animal Care and Use Committee of Institute of Oceanology, Chinese Academy of Sciences.

Artificially induced polyploid and gynogenetic flounder

The artificial induction of polyploid and gynogenetic flounder were performed in Shenghang Fish Farm (Weihai, China). The triploid induction was induced by cold shock technique using previously described methods (You et al. 2001), the tetraploid group was induced by hydrostatic pressure shock under 60 MPa at 10 min before the first cleavage for 6 min, and a diploid control was set to assess the fertilization capability of the gametes. The meiogynogenetic diploid and mitogynogenetic diploid groups were induced, and a diploid control and a haploid control were simultaneously set as previous reported (Wang et al. 2008; You et al. 2008a). The cross was performed using eggs and sperm from a single female and a single male. The embryos of each group were obtained from three different crosses. The produced progenies were incubated in nets floating in a 16-m^3 water pool under controlled conditions (L:D, 14:10; 15.0 ± 1.0 °C; 30 ‰; aeration). The triploidy and tetraploidy were determined in embryos by karyotyping of about 200 gastrulae (You and Liu 1995), and the gynogenetic induction groups were determined in embryos by morphologic observation (You et al. 2008b).

Sample collection and fixation

Six representative embryonic stages were randomly and carefully selected for investigating *pax3a* and *pax3b* expression by whole-mount in situ hybridization. These six stages were kupffer's vesicle (KV) formation stage (no somite formation), blastopore closure stage (4–6 somites), tailbud formation stage (about 14 somites), 25 somites stage, embryo encircling 4/5 of the yolk sac stage, and hatching stage, which were sequentially named as stages 1, 2, 3, 4, 5, and 6. About 300 embryos were fixed with 4 % paraformaldehyde (Sigma, St Louis, MO, USA) in PBS (4 % PFA) and then transferred into absolute methanol for long-term storage.

Whole-mount in situ hybridization

One-color in situ hybridization was performed with digoxigenin-labeled *pax3a* or *pax3b* antisense riboprobe as described previously (Jiao et al. 2015). Images were captured with a Leica DFC420C camera mounted on a Leica DMLB2 microscope (Leica, Wetzlar, Germany). Embryos in the diploid control group developed normally and had normal *pax3a* and *pax3b* expression patterns. In this paper, we classified normal or abnormal embryos based on *pax3a* and *pax3b* expression patterns compared with their expression patterns in the diploid control group.

Data handling

Two hundred embryos from each group were incubated in an incubator under controlled conditions to calculate the fertilization rate and hatching rate. Differences between experimental groups were analyzed using Student's *t* test. The calculation formulas are as follows (ref):

$$\text{Fertilization rate}\,(\%) = \text{Embryonic buoyant eggs at the blastula stage/Initial buoyant eggs after induction} \times 100\,\%.$$

$$\text{Hatching rate}\,(\%) = \text{Newly hatched larvae/Initial buoyant eggs after induction} \times 100\,\%.$$

$$\text{The gynogenetic induction rate}\,(\%) = \text{The number of successfully induced embryos (or larvae)}/\text{Total embryos (or larvae) number} \times 100\,\%.$$

$$\text{The polyploidy induction rate}\,(\%) = \text{The number of karyotypes with expected chromosome number/The number of total karyotypes} \times 100\,\%.$$

Results

Localization of *pax3a* and *pax3b* mRNA in embryos of the diploid control, and triploid, tetraploid induction groups

The mean artificial fertilization rates of triploid, tetraploid induction groups, and diploid controls were 28.26, 48.15, and 62.22 %, respectively. Their corresponding mean hatching rates were 8.76, 10.59, and 46.67 % (Table 1). At hatching stage, the induction rate of the triploid group reached 100 %, and that of the tetraploid group was about 70–80 %. Then, we performed whole-mount in situ hybridization for analysis of *pax3a* and *pax3b* expression during embryogenesis.

Figure 1 showed the expression patterns of *pax3a* mRNA in diploid, triploid, and tetraploid groups during embryogenesis. The results revealed that the *pax3a* gene was expressed in the neural plate, the brain region, and was also scattered in the somites in the diploid control group (Fig. 1a1–a6). A similar expression pattern was observed in 90.47 % of embryos in the triploid group (Fig. 1b1–b6), and 82.28 % of embryos in the tetraploid group (Fig. 1c1–c6). Few embryos in these two groups showed abnormal or delayed expression of *pax3a* (Fig. 3b′, c′). For the tetraploid induction group, after correction of its induction rate (70–80 %), the percentages of normal *pax3a*-expressing embryos from stages 1 to 6 were about 70–80, 70–80, 43.75–50, 53.53–61.18, 54.45–62.22 and 53.84–61.54 % sequentially.

To further confirm the results from *pax3a* signals, we also detected *pax3b* mRNA signals in these groups and got consistent results (Fig. 2). The *pax3b* gene expression was detected in the neural plate, the brain region, and the newly forming somites in the diploid control group (Fig. 2a1–a6). In the triploid and tetraploid induction groups, 96.54 and 77.59 % of embryos displayed normal signals for the *pax3b* gene, respectively (Fig. 2b1–b6, c1–c6). Also, few embryos in these two groups showed abnormal or delayed expression of *pax3b* (Fig. 3b″, c″). For the tetraploid induction group, after correction of its induction rate (70–80 %) the percentages of normal *pax3b*-expressing embryos from stages 1 to 6 were 63.64–72.73, 60–68.57, 42–48, 54.45–62.22, 54.45–62.22 and 51.33–58.66 % sequentially.

Localization of *pax3a* and *pax3b* mRNA in embryos of the diploid control, and gynogenetic haploid, meiogynogenetic diploid, mitogynogenetic diploid induction groups

The mean artificial fertilization rates of gynogenetic haploid, meiogynogenetic diploid, mitogynogenetic diploid groups, and their diploid control groups were 81.23, 48.90, 81.03, and 67.80 %, respectively. Their corresponding mean hatching rates were 0, 20.97, 26.44, and 51.76 % (Table 2). At hatching stage, the induction rates of gynogenetic haploid, meiogynogenentic diploid, and mitogynogenetic diploid groups reached 100 %.

The *pax3a* mRNA signals were detected by whole-mount in situ hybridization during early development (Fig. 4). In the diploid control group, *pax3a* mRNA displayed normal expression patterns in the brain and trunk regions (Fig. 4a1–a6). However, in the gynogenetic haploid group, almost all embryos showed typical haploid syndrome with abnormal expression of *pax3a* in the brain and trunk regions (Fig. 4b1–b6). 85.29 % of embryos in the meiogynogenetic diploid group had normal expression of *pax3a* as in the diploid control group (Fig. 4c1–c6). In the mitogynogenetic

Table 1 Fertilization rates and hatching rates of diploid control and polyploid induction groups

	2*n*	3*n*	4*n*
Fertilization rate (%)	62.22 ± 7.93	28.26 ± 8.58**	48.15 ± 4.63*
Hatching rate (%)	46.67 ± 3.62	8.76 ± 1.46**	10.59 ± 1.18**

The results were subjected to t test analysis, values are presented as mean ± SD ($n = 3$)

2n diploid control, *3n* triploid induction group, *4n* tetraploid induction group

* Significant different from diploid control, $P < 0.05$

** Extremely significant different from diploid control, $P < 0.01$

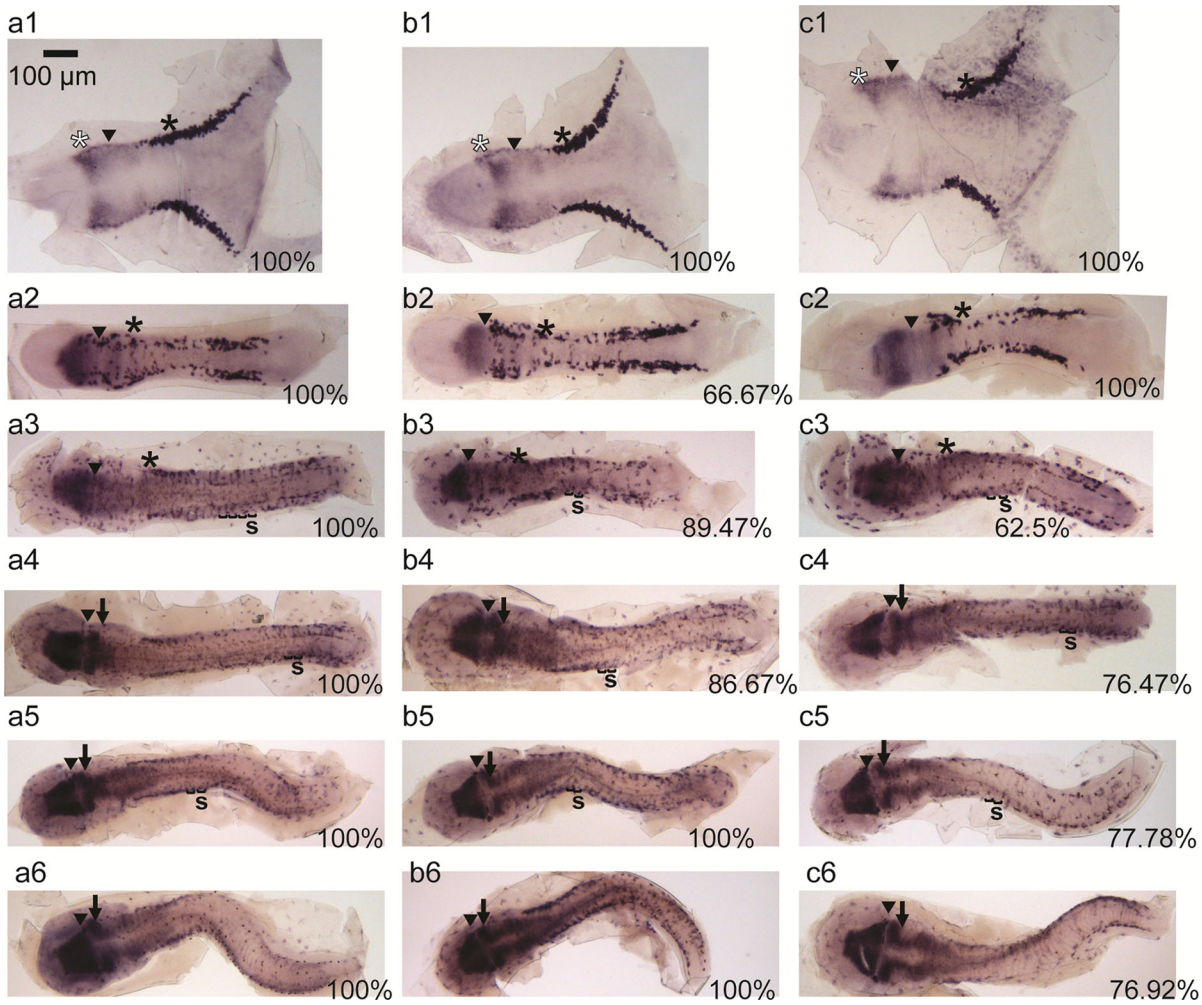

Fig. 1 Detection of *pax3a* mRNA expression in the diploid control, and the triploid, and tetraploid induction groups during embryogenesis by whole-mount in situ hybridization. *Head to the left*, dorsal view. **a1**–**a6**, diploid control (2*n*). **b1**–**b6**, triploid induction group (3*n*). **c1**–**c6**, tetraploid induction group (4*n*). 1–6, embryos at stages 1 to 6 in sequence. 30 embryos from each stage were scored, and data are shown as a percentage in the *right corner*. *Black arrowhead* indicates isthmus of decreasing *pax3a* expression that separates midbrain and hindbrain boundary. *Black arrow* indicates the primordial cerebellum. *Black asterisk* indicates the lateral neural plate. *White asterisk* indicates cranial neural crest (NC). A *black bracket* indicates a somite. *Bars* 100 μm

diploid group, 66.66 % of embryos had abnormal expression of *pax3a*, similar to the gynogenetic haploid group despite displaying less severe symptoms (Fig. 4d1–d6). Besides, the abnormal *pax3a*-expressing embryos of the gynogenetic haploid group and mitogynogenetic diploid group had specific abnormal expression patterns of *pax3a*, showing cross-shaped signals in the brain and bilateral signals in the trunk (Fig. S1).

Figure 5 showed the expression of *pax3b* mRNA in these groups and the result was similar. In the diploid control group, *pax3b* was expressed normally in the brain and trunk regions despite very few embryos (12.5 %) showing abnormal *pax3b* signals at the fourth stage (Fig. 5a1–a6). In the gynogenetic haploid group, all embryos showed typical haploid syndrome with abnormal expression of *pax3b* (Fig. 5b1–b6). 87.94 % of embryos in the meiogynogenetic diploid group had normal expression of *pax3b* as in the diploid control group (Fig. 5c1–c6). In the mitogynogenetic diploid group, 58.97 % of embryos had abnormal expression of

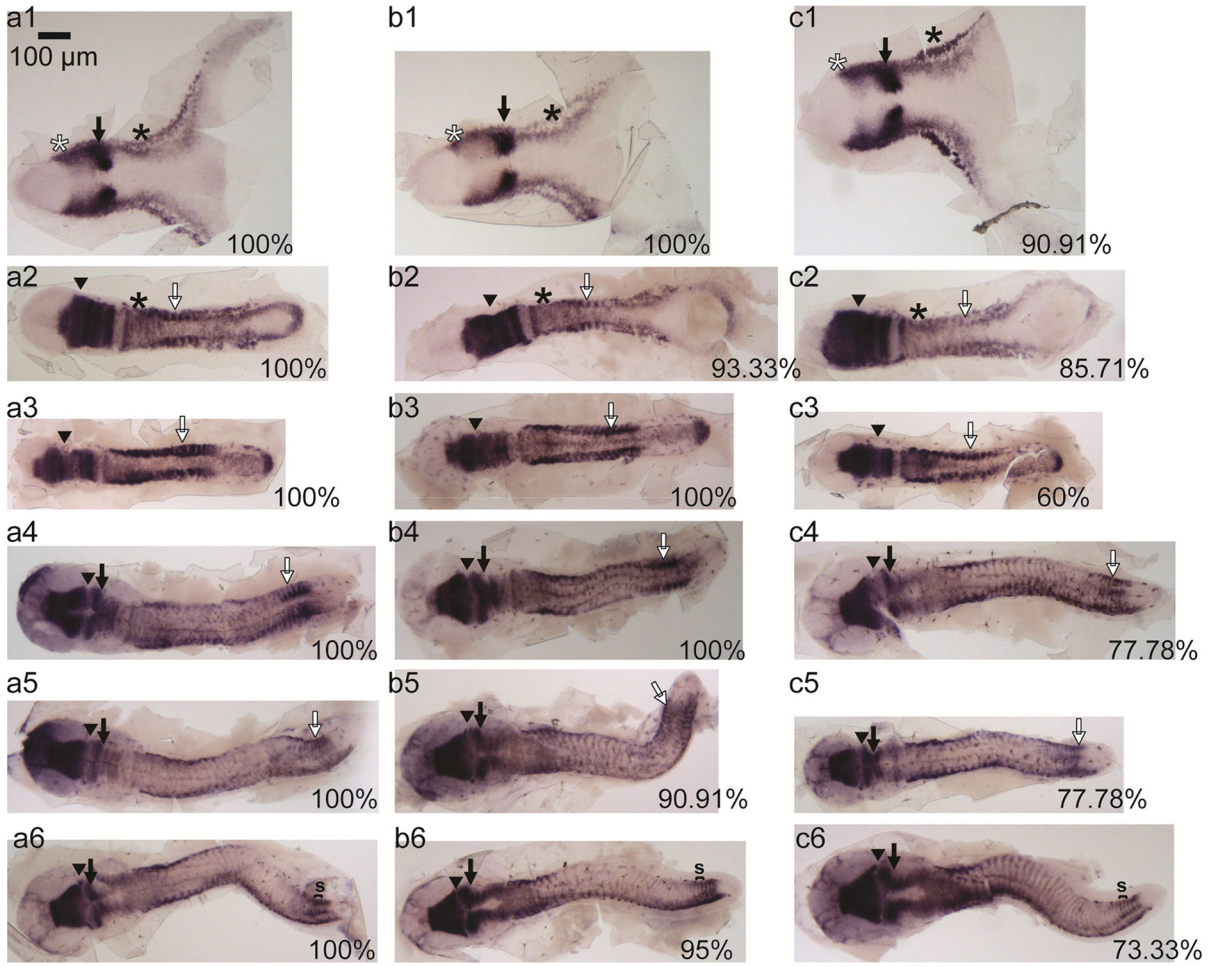

Fig. 2 Detection of *pax3b* mRNA expression in the diploid control, and the triploid, and tetraploid induction groups during embryogenesis by whole-mount in situ hybridization. *Head to the left*, dorsal view. **a1**–**a6**, diploid control (2*n*). **b1**–**b6**, triploid induction group (3*n*). **c1**–**c6**, tetraploid induction group (4*n*). 1–6, embryos at stages 1 to 6 in sequence. 30 embryos from each stage were scored and, data are shown as a percentage in the *right corner*. *Black arrowhead* indicates isthmus of decreasing *pax3b* expression that separates midbrain and hindbrain boundary. *Black arrow* indicates the primordial cerebellum. *Black asterisk* indicates the lateral neural plate. *White arrow* indicates the newly forming somites. *White asterisk* indicates cranial neural crest (NC). *Bars* 100 μm

pax3b, similar to the gynogenetic haploid group despite displaying less severe symptoms (Fig. 5d1–d6). Besides, the abnormal expression patterns of *pax3b* in the embryos of the gynogenetic haploid group and mitogynogenetic diploid group were both specific (Fig. S2). In the abnormal *pax3b*-expressing embryos of the gynogenetic haploid group, *pax3b* showed cross-shaped signals in the brain region and strong bilateral signals in the somites. Similarly, in the abnormal *pax3b*-expressing embryos of the mitogynogenetic diploid group, abnormal expression of *pax3b* was also found in the brain region and somites, although with microcephaly in the late stages.

Discussion

Here we compared the expression patterns of the *pax3a* and *pax3b* genes in polyploid induction groups and their diploid controls during embryogenesis by whole-mount in situ hybridization. The results showed that the artificial induction of triploidy had a small

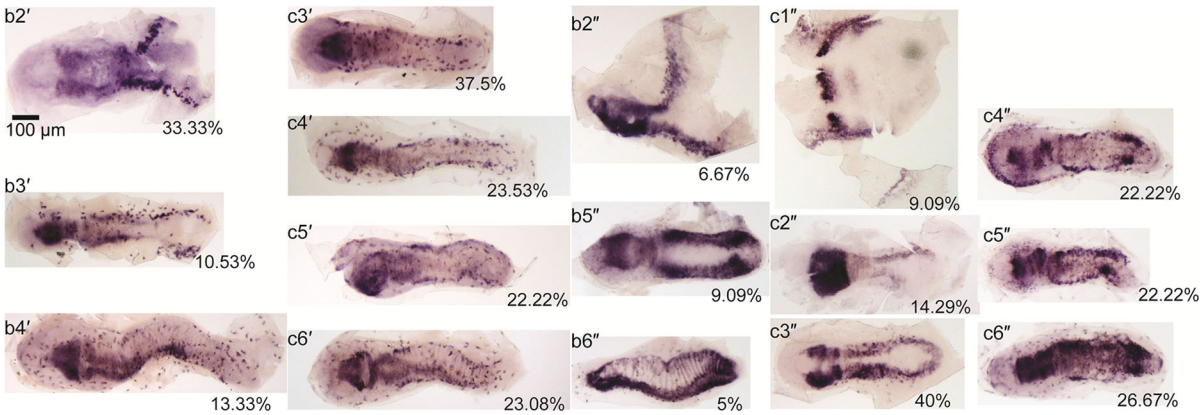

Fig. 3 Abnormal expression of *pax3a/3b* mRNA in the ploidy-manipulated groups during embryogenesis by whole-mount in situ hybridization. *Head to the left*, dorsal view. In order to keep in line with Figs. 1 and 2, b and c indicate triploid and tetraploid induction groups, respectively. 1–6, embryos at stages 1 to 6 in sequence. The prime symbol (′) and double prime symbol (″) indicate *pax3a* and *pax3b* mRNA in situ hybridization results, respectively. 30 embryos from each stage were scored, and data are shown as a percentage in the *right corner*

Table 2 Fertilization rates and hatching rates of diploid control and gynogenetic induction groups

	2*n*	*n*	MeG2n	MiG2n
Fertilization rate (%)	67.80 ± 16.68	81.23 ± 0.49	48.90 ± 14.61	81.03 ± 1.45
Hatching rate (%)	51.76 ± 14.60	0	20.97 ± 4.40**	26.44 ± 12.50*

The results were subjected to *t* test analysis, values are presented as mean ± SD ($n = 3$)

2n diploid control, *n* gynogenetic haploid induction group, *MeG2n* meiogynogenetic diploid induction group, *MiG2n* mitogynogenetic diploid induction group

* Significant different from diploid control, $P < 0.05$

** Extremely significant different from diploid control, $P < 0.01$

effect on *pax3a* and *pax3b* gene expression patterns; however, the artificial induction of tetraploidy caused 45 % abnormal *pax3a/3b*-expressing embryos from stages 3 to 6.

Previous studies have focused on methods to produce polyploidy, identify polyploidy, and determine growth characteristics of polyploid fish using the phenotype observation method (Liu et al. 2008; Xu and Chen 2010; Yi et al. 2012; You and Liu 1995; You et al. 2001). In this work, we found that most embryos of the triploid induction group developed morphologically normal compared with the diploid control. More importantly, 94 % of embryos had normal expression patterns of *pax3a* and *pax3b* mRNA during embryogenesis. Thus, the induction of triploidy by chromosome set manipulation had a small effect on neurogenesis and myogenesis in flounder embryos. However, induction of tetraploidy had a moderate effect on the embryonic neurogenesis and myogenesis, causing 45 % abnormal *pax3a/3b*-expressing embryos. Compared with *pax3a*, *pax3b* displayed more evident expression signals in the brain and somite regions with some subtle regional differences. As shown in Fig. 3, in the tetraploid induction group, *pax3b* signals in the brain region remained in the cranial neural crest and lateral neural plate which may impede the normal development of the neural tube and brain. Besides, the body length became shorter with abnormal expression patterns of *pax3b* in the somites, indicating that myogenesis may be affected. The stability of polyploids depended on rapid genome recombination and changes in gene expression after formation (Song et al. 2012). Genome sequencing and related molecular systematics and bioinformatics studies on polyploids will be a new way to identify the involved genes and signal transduction pathways.

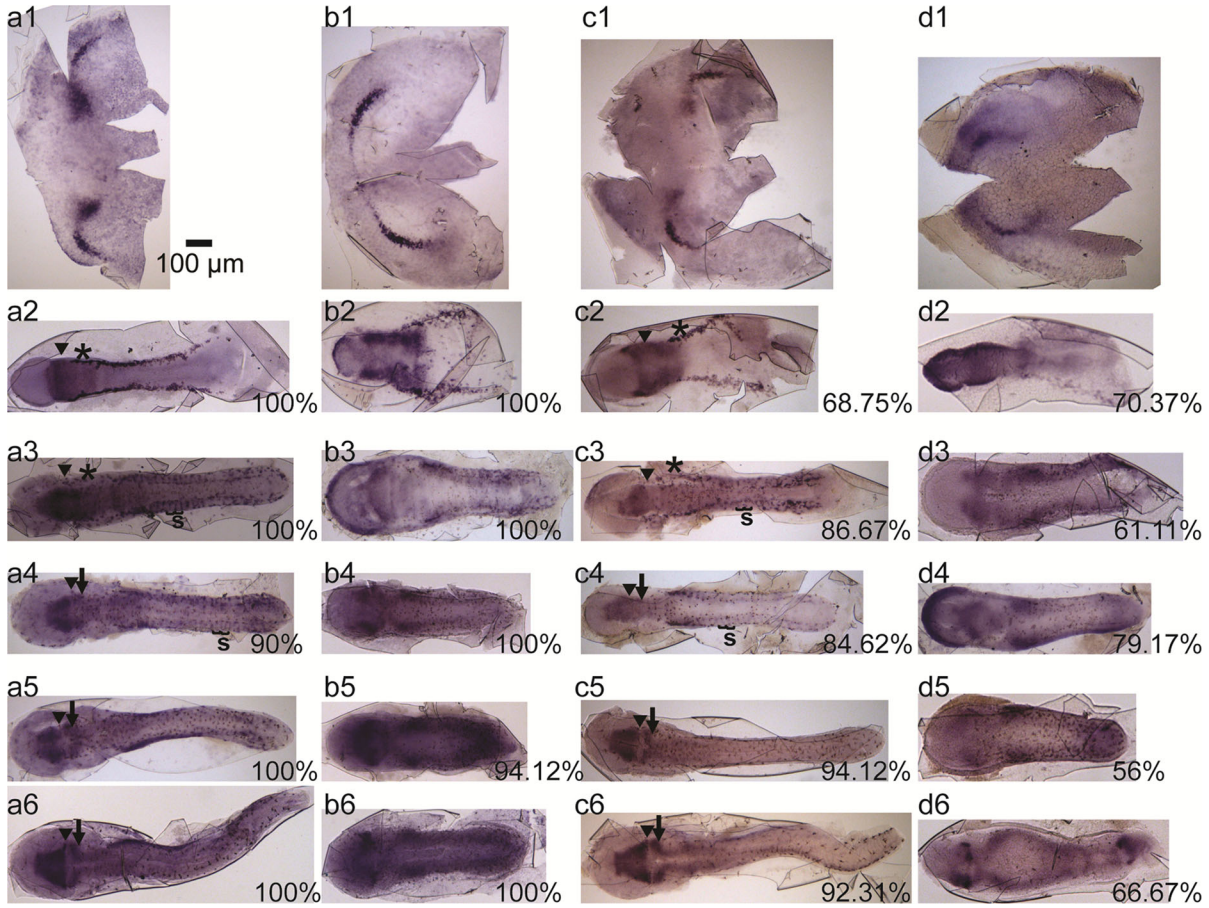

Fig. 4 Detection of *pax3a* mRNA expression in the diploid control, and the gynogenetic haploid, meiogynogenetic diploid, and mitogynogenetic diploid induction groups during embryogenesis by whole-mount in situ hybridization. *Head to the left*, dorsal view. **a1**–**a6**, diploid control (2*n*). **b1**–**b6**, gynogenetic haploid induction group (*n*). **c1**–**c6**, meiogynogenetic diploid induction group (MeG2n). **d1**–**d6**, mitogynogenetic diploid induction group (MiG2n). 1–6, embryos at stages 1 to 6 in sequence. 30 embryos from each stage were scored, and data are shown as a percentage in the *right corner*. As the in situ hybridization signals at stage 1 were difficult to identify, we did not count the results of the period. *Black arrowhead* indicates isthmus of decreasing *pax3a* expression that separates midbrain and hindbrain boundary. *Black arrow* indicates the primordial cerebellum. *Black asterisk* indicates the lateral neural plate. *White asterisk* indicates cranial neural crest (NC). A *black bracket* indicates a somite. *Bars* 100 μm

Research showed nutrient regulatory mechanisms in skeletal muscle, including those affecting proteolysis, differed between diploid and triploid juvenile rainbow trout (*O. mykiss*) during recovery from feed deprivation. Since the rate of protein accumulation in skeletal muscle largely determined growth rate, chromosome set manipulation might affect the growth rate through this process (Cleveland and Weber 2013). Also in juvenile rainbow trout, polyploidy influenced the expression of genes critical to muscle development and general growth regulation, which may explain why triploid fish recover from nutritional insult better than diploid fish (Cleveland and Weber 2014). So it stands to reason that the muscle development will be affected in the polyploid juvenile flounder, and further studies are needed to assess this benefit.

In this study, we also compared the expression patterns of *pax3a* and *pax3b* genes in gynogenetic induction groups and their diploid control during embryogenesis by whole-mount in situ hybridization. Almost 100 % of embryos in the gynogenetic haploid induction group and 63 % of embryos in the mitogynogenetic diploid induction group showed abnormal *pax3a* and *pax3b* expression patterns, with impaired

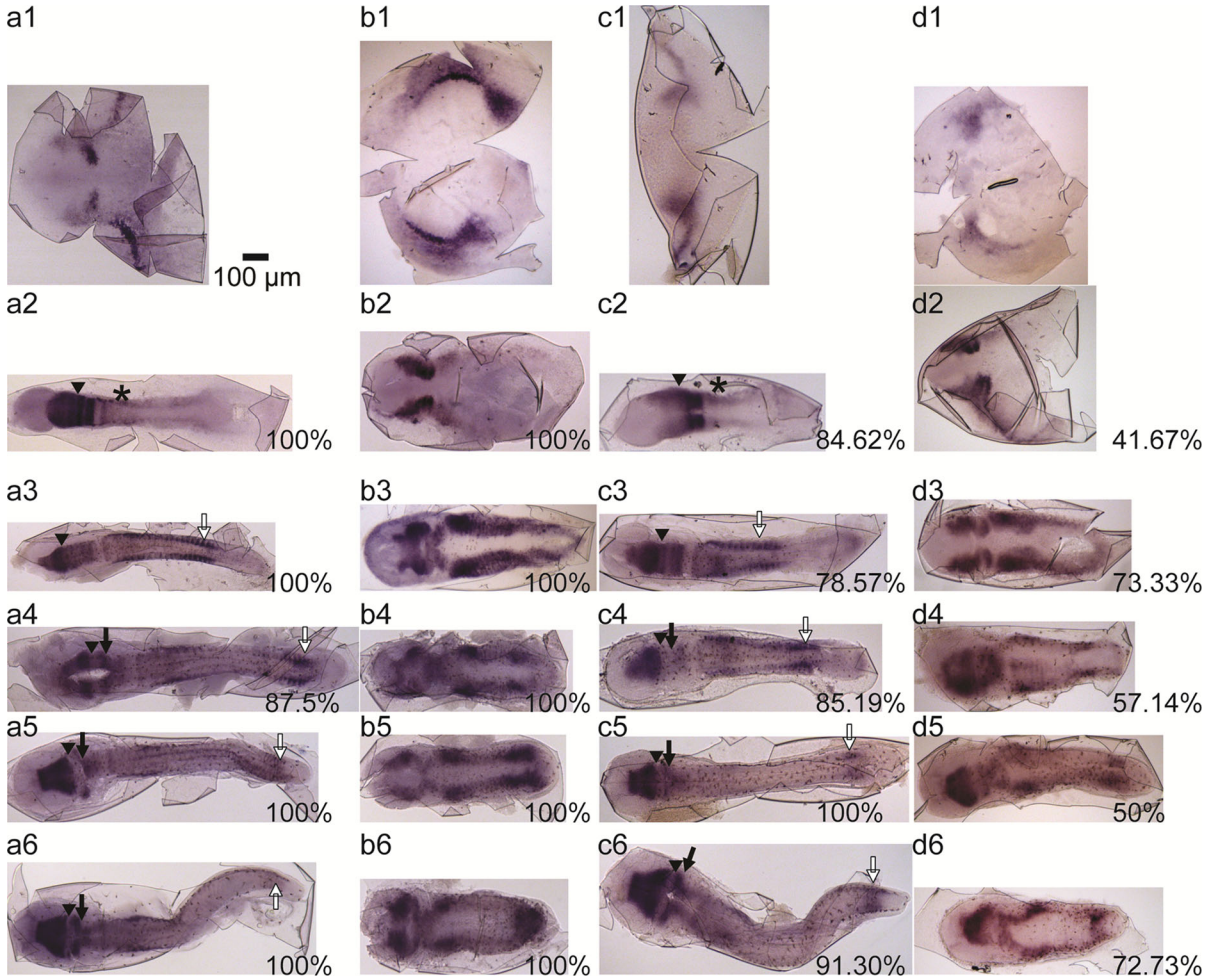

Fig. 5 Detection of *pax3b* mRNA expression in the diploid control, and the gynogenetic haploid, meiogynogenetic diploid, and mitogynogenetic diploid induction groups during embryogenesis by whole-mount in situ hybridization. *Head to the left*, dorsal view. **a1**–**a6**, diploid control (2*n*). **b1**–**b6**, gynogenetic haploid induction group (*n*). **c1**–**c6**, meiogynogenetic diploid induction group (MeG2n). **d1**–**d6**, mitogynogenetic diploid induction group (MiG2n). 1–6, embryos at stages 1 to 6 in sequence. 30 embryos from each stage were scored, and data are shown as a percentage in the *right corner*. As the in situ hybridization signals at stage 1 were difficult to identify, we did not count the results of the period. *Black arrowhead* indicates isthmus of decreasing *pax3b* expression that separates midbrain and hindbrain boundary. *Black arrow* indicates the primordial cerebellum. *White arrow* indicates the newly forming somites. *Black asterisk* indicates the lateral neural plate. *White asterisk* indicates cranial neural crest (NC). *Bars* 100 μm

neural development and short myotomes. In spite of this, about 87 % of embryos in the meiogynogenetic diploid group showed normal expression patterns of the *pax3a* and *pax3b* genes.

Flounder embryos of the gynogenetic haploid group developed the typical haploid syndrome (impaired neural development, short myotomes, microcephalic, lordosis, and poor muscle differentiation) as described in the literature (Hamilton 1963, 1966; Purdom 1969). There were some explanations of the development of the haploid syndrome, such as nucleocytoplasmic imbalance, unmasked recessive lethal genes, and lack of heterozygosity (Hamilton 1966). In goldfish, some differentially expressed proteins were found between diploid embryos and haploid embryos, in which some proteins were related with eye development, nerve development, developmental regulation, cell differentiation, and signal transduction (Huang et al. 2004). But, the predictions need to be confirmed in the future.

Our data were consistent with previous results showing that meiogynogenetic diploids develop normally compared with the diploid control group from the gastrula stage to the hatching stage. There were no significant differences in the growth of the meiogynogenetic diploid experimental group larvae and the control group larvae (You et al. 2001). Moreover, our data further demonstrated that the early neural and muscle development were not affected by artificially induced meiogynogenesis. On the contrary, embryos of the mitogynogenetic diploid induction group displayed severely aberrant neural and muscular development. The possible reasons for these phenomena might be: (1) embryos of meiogynogenetic diploid induction group retain significant levels of heterozygosity depending on the degree of crossing-over between homologous chromosomes during meiosis I, whereas embryos of mitogynogenetic diploid induction group are theoretically homozygous at every loci, which include dominance of recessive lethal genes leading to a significant reduction in the survival rate (Felip et al. 2001); (2) the timing of diploidization of chromosome set in mitogynogenesis is later than in meiogynogenesis, which might cause the asynchrony of embryonic development during mitogynogenetic induction, and more severe damage to embryogenesis (Chen et al. 2012).

In conclusion, the expression patterns of *pax3a* and *pax3b* during embryogenesis were comparatively analyzed in the artificially induced polyploidy and gynogenesis in flounder. Differential expression patterns were discovered. The abnormal ratios of *pax3a/3b* expressing embryos in the triploid induction group, tetraploid induction group, gynogenetic haploid induction group, meiogynogenetic diploid induction group, and mitogynogenetic diploid induction group were 6, 40, 99, 13, and 63 % in sequence. The abnormal expression patterns of *pax3a/3b* in the tetraploid induction group were not specific, showing delayed or abnormal expression in the brain, and disordered signals in the trunk. The abnormal expression patterns of *pax3a/3b* in the gynogenetic haploid induction group and mitogynogenetic diploid induction group were both specific, mainly showing cross-shaped signals in the brain and abnormal bilateral signals in the trunk. Therefore, we preliminarily considered that the *pax3a* and *pax3b* could be used as molecular markers to assess normal or abnormal embryonic neurogenesis and myogenensis in flounder. Our findings will have both important theoretical significance and valuable applications.

Acknowledgments We thank Dr. Erik Anderson for proofreading this manuscript. This work was supported by the National High Technology Research and Development Program of China (863 Program) (No. 2012AA10A402), the Natural Science Foundation of China (NSFC, 31502146 and 31502156), the Shandong Provincial Natural Science Foundation, China (BS2014HZ008), and the Scientific and Technological Innovation Project Financially Supported by Qingdao National Laboratory for Marine Science and Technology (No. 2015ASKJ02).

References

Buckingham M, Relaix F (2015) PAX3 and PAX7 as upstream regulators of myogenesis. Semin Cell Dev Biol 44:115–125

Chen SL, Ji XS, Shao CW, Li WL, Yang JF, Liang Z et al (2012) Induction of mitogynogenetic diploids and identification of WW super-female using sex-specific SSR markers in half-smooth tongue sole (*Cynoglossus semilaevis*). Mar Biotechnol (NY) 14:120–128

Cleveland BM, Weber GM (2013) Effects of triploidy on growth and protein degradation in skeletal muscle during recovery from feed deprivation in juvenile rainbow trout (*Oncorhynchus mykiss*). Comp Biochem Physiol A Mol Integr Physiol 166:128–137

Cleveland BM, Weber GM (2014) Ploidy effects on genes regulating growth mechanisms during fasting and refeeding in juvenile rainbow trout (*Oncorhynchus mykiss*). Mol Cell Endocrinol 382:139–149

Felip A, Zanuy S, Carrillo M, Piferrer F (2001) Induction of triploidy and gynogenesis in teleost fish with emphasis on marine species. Genetica 111:175–195

Hamilton L (1963) An experimental analysis of the development of the haploid syndrome in embryos of *Xenopus laevis*. J Embryol Exp Morphol 11:267–278

Hamilton L (1966) The role of the genome in the development of the haploid syndrome in Anura. J Embryol Exp Morphol 16:559–568

Huang L, Li B, Luo C, Xie J, Chen P, Liang S (2004) Proteome comparative analysis of gynogenetic haploid and diploid embryos of goldfish (*Carassius auratus*). Proteomics 4:235–243

Jiao S, Tan X, Wang Q, Li M, Du SJ (2015) The olive flounder (*Paralichthys olivaceus*) Pax3 homologues are highly conserved, encode multiple isoforms and show unique expression patterns. Comp Biochem Physiol B Biochem Mol Biol 180:7–15

Johnston IA, Strugnell G, McCracken ML, Johnstone R (1999) Muscle growth and development in normal-sex-ratio and all-female diploid and triploid Atlantic salmon. J Exp Biol 202:1991–2016

Lang D, Powell SK, Plummer RS, Young KP, Ruggeri BA (2007) PAX genes: roles in development, pathophysiology, and cancer. Biochem Pharmacol 73:1–14

Li M, Tan X, Jiao S, Wang Q, Wu Z, You F et al (2015) A new pattern of primordial germ cell migration in olive flounder (*Paralichthys olivaceus*) identified using nanos3. Dev Genes Evol 225:195–206

Liu HJ, Wang CA, Zhu XC, Liu YX, Zhang XY, Hou JL et al (2008) Embryonic development of gynogenetic diploid and triploid Japanese flounder *Paralichthys olivaceus*. J Dalian Fish Univ 23:161–167 **(in Chinese with English abstract)**

Minchin JE, Hughes SM (2008) Sequential actions of Pax3 and Pax7 drive xanthophore development in zebrafish neural crest. Dev Biol 317:508–522

Minchin JE, Williams VC, Hinits Y, Low S, Tandon P, Fan CM et al (2013) Oesophageal and sternohyal muscle fibres are novel Pax3-dependent migratory somite derivatives essential for ingestion. Development 140:2972–2984

Molina-Luzon MJ, Lopez JR, Robles F, Navajas-Perez R, Ruiz-Rejon C, De la Herran R et al (2015) Chromosomal manipulation in Senegalese sole (*Solea senegalensis* Kaup, 1858): induction of triploidy and gynogenesis. J Appl Genet 56:77–84

Purdom CE (1969) Radiation-induced gynogenesis and androgenesis in fish. Heredity (Edinb) 24:431–444

Relaix F, Rocancourt D, Mansouri A, Buckingham M (2004) Divergent functions of murine Pax3 and Pax7 in limb muscle development. Genes Dev 18:1088–1105

Schubert FR, Tremblay P, Mansouri A, Faisst AM, Kammandel B, Lumsden A et al (2001) Early mesodermal phenotypes in splotch suggest a role for Pax3 in the formation of epithelial somites. Dev Dyn 222:506–521

Seo HC, Drivenes O, Ellingsen S, Fjose A (1998) Transient expression of a novel Six3-related zebrafish gene during gastrulation and eye formation. Gene 216:39–46

Song C, Liu S, Xiao J, He W, Zhou Y, Qin Q et al (2012) Polyploid organisms. Sci China Life Sci 55:301–311

Tremblay P, Kessel M, Gruss P (1995) A transgenic neuroanatomical marker identifies cranial neural crest deficiencies associated with the Pax3 mutant Splotch. Dev Biol 171:317–329

Uwa H (1965) Gynogenetic haploid embryos of the medaka (*Oryzias latipes*). Embryologia (Nagoya) 9:40–48

Wang W, You F, Xu J, Sun W, Zhu X, Gao T et al (2008) Genetic analysis of meio- and mito-gynogenetic stocks of the with *Paralichthys olivaceus* microsatellite markers. Acta Oceanologica Sinica 27:149–156

Xu TJ, Chen SL (2010) Induction of All-triploid Japanese Flounder (*Paralichthys olivaceus*) by Cold Shock. Isr J Aquacult-Bamidgeh 62:43–49

Xu K, Duan W, Xiao J, Tao M, Zhang C, Liu Y et al (2015) Development and application of biological technologies in fish genetic breeding. Sci China Life Sci 58:187–201

Yi QL, Yu HY, Wang XL, Wang ZG, Wang XB, Qi J et al (2012) Production of viable tetraploid olive flounder (*Paralichthys olivaceus*) by hydrostatic pressure shock. Oceanol Limnol Sin 43:382–388

You F, Liu J (1995) Karyotype evidences of triploidy in the left-eyed flounder, *Paralichthys olivaceus* (T. & S.). Oceanol Limnol Sin Suppl 26:115–118 **(in Chinese with English abstract)**

You F, Liu J, Wang XC, Xu YL, Huang RD, Zhang PJ (2001) Study on embryonic development and early growth of triploidand gynogenetic diploid left—eyed flounder, *Paralichthys olivaceus* (T. et S.). Chin J Oceanol Limnol 19:147–151

You F, Xu JH, Ni J, Sun W, Zhu XP, Xu DD et al (2008a) Study on artificial induction of mitogynogenetic diploid in *Paralichthys olivaceus*. High Technol Lett 18:874–880 **(in Chinese with English abstract)**

You F, Xu JH, Zhu XP, Xu YL, Zhang PJ (2008b) Effect of ultraviolet irradiation on sperm of the left-eyed flounder, *Paralichthys olivaceus*. J World Aquacult Soc 39:414–422